IEEE Access
Multidisciplinary : Rapid Review : Open Access Journal

Received 25 September 2023, accepted 21 October 2023, date of publication 2 November 2023,
date of current version 8 November 2023.

Digital Object Identifier 10.1109/ACCESS.2023.3329681

RESEARCH ARTICLE

Design of a Hybrid Radar Sensor to Monitor the Behavior of a Projectile in a Circular Tube

MYUNG-SUK JUNG[1,2], JAE-HYUN CHOI[2], MIN-SUP SONG[2], JIN-EEP ROH[2], AND KYUNG-TAE KIM[1], (Member, IEEE)
[1]Department of Electrical Engineering, Pohang University of Science and Technology, Pohang 37673, South Korea
[2]Agency for Defense Development, Yuseong, Daejeon 34186, South Korea

Corresponding author: Kyung-Tae Kim (kkt@postech.ac.kr)

This work was supported by the Agency for Defense Development Grant funded by the Korean Government under Grant 954013001.

ABSTRACT This study proposes a hybrid radar sensor that can monitor the behavior of projectiles in near real-time in a soft recovery system (SRS) to verify the high-impact characteristics of key components in smart ammunitions. The sensor comprises a frequency-modulated continuous wave (FMCW) radar mode to check whether the soft recovery of the projectile is normal after being launched and a CW Doppler radar mode to estimate the projectile velocity, distance traveled, and deceleration characteristics during the test. As the proposed sensor is installed inside a 155.8 mm circular tube, 1.4 GHz is chosen as the operating frequency to ensure that the sensor only operates in the dominant mode. Moreover, the radar equations in free space are modified to consider radar operation inside the tube and ensure accurate calculations. A hybrid radar sensor is installed and operated inside an SRS test device. The position of the projectile after the test is determined from the positions of the peaks of the receiving signals in the FMCW mode. The projectile velocity, traveling distance, and decay velocity are accurately predicted using the CW Doppler mode.

INDEX TERMS CW Doppler radar, FMCW radar, hybrid sensor, SRS.

I. INTRODUCTION

With the recent development of guided missiles and smart munitions, electronic components, such as drive systems, global positioning systems (GPS), guidance systems, and electronic fuzes, are now being installed inside guided missiles and munitions. However, unlike guided missiles, which have a backward inertia of a few tens of g (acceleration due to gravity), smart munitions are subjected to high backward inertial forces of up to 15,000 g upon the initial launch, requiring high impact resistance properties for their embedded components [1], [2].

Therefore, firing tests are essential for verifying the impact resistance properties of components in smart munitions. In an actual firing, it is difficult to retrieve fired projectiles to check the status of the internal components; even if retrieval is possible, it is difficult to distinguish whether the failure occurred during firing or upon impact with the target or ground. To solve this problem, various methods have been proposed to safely retrieve projectiles without impacts other than firing [3], [4], [5], [6], [7], [8].

In the ballistic rail gun test [3], [4], a test shell with a water-scoop shape, instead an ogive nose, was fired into an inclined water-filled tube, and the interaction between the water scoop and water in the tube resulted in soft recovery. The test shell characteristics were obtained using a frequency-modulated (FM) telemetry transmitter mounted on a water scoop, which transmitted real-time acceleration, pressure, and strain sensor signals in the shell cavity. This method advantageously recovers the shell at a short distance but can only test the impact immunity of the devices or internal components.

Chung et al. [5] proposed a method in which a projectile slowed as it passed through multiple thin metal plates for soft recovery. The projectile velocity was measured based on the breakage time of the thin aluminum plates and the position of each aluminum plate. However, their method is time consuming and expensive, and unwanted loads are imposed on the test projectile. Therefore, ballistic compression decelerators

The associate editor coordinating the review of this manuscript and approving it for publication was Wen-Sheng Zhao.

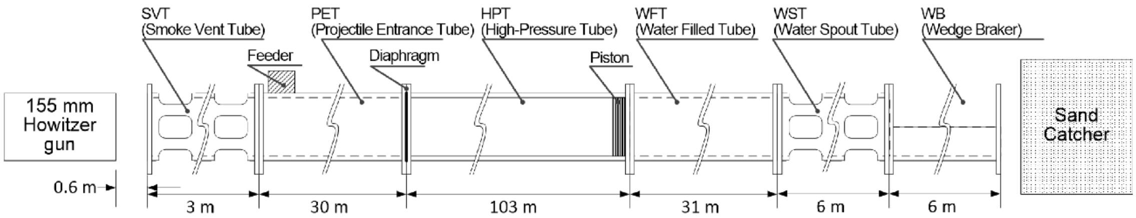

FIGURE 1. Configuration of the SRS.

are preferable [6], [7]. These soft recovery system (SRS) tests facilitate the conduction of many test trials using projectiles equipped with onboard recorders [8], [9], [10], comprising single-or multichannel accelerometers and data recorders, to establish the launch conditions of the projectile before the actual shell test. Onboard recorders provide an accurate view of both the launch and in-tube behaviors.

However, they require a large amount of time to verify the data after the test, which is disadvantageous because they have the possibility of being damaged by excessively high-impact test conditions after a few repeated tests. Hence, real-time verification cannot be performed using onboard recorders. Real-time data measurements in the shell can be performed using laser telemetry [11]. This method requires a mirror and lens in front of the muzzle to receive the telemetry signal. However, it can cause damage during testing.

In this study, a hybrid radar sensor [12] with a frequency-modulated continuous-wave (FMCW) radar mode and a CW Doppler radar mode is proposed to measure the behavior of a projectile moving in the tube of an SRS device. The velocity of the test projectile was measured in real time using actual test data. The proposed sensor can be used semipermanently, and the behavioral characteristics of the projectile can be checked immediately after the test, drastically reducing the time between multiple tests and the number of pretests to ensure good test conditions.

CW Doppler radars have been employed to analyze the behavior of artillery shells [3], [4], [13], [14], [15]. However, the methods reported in [3], [4], and [13] were used to monitor behavior in free space after muzzle departure, instead of inside the tube. In [14] and [15], a W-band high-frequency Doppler radar was adopted; the approach in [14] was only applicable to systems with an open rear, such as rail guns. In [15], similar to [11], a metal plate that reflected radio waves was placed in front of the muzzle to measure in-cavity behavior. However, the method is not applicable to the SRS system in this study because the SRS tube is long and contains a diaphragm and a piston.

In Chapter II, the feeder of the monitor sensor and design of the proposed hybrid radar sensor are described. In Chapter III, the measured characteristics of the fabricated monitor sensor are presented, and the results of the SRS test using the fabricated hybrid radar sensor are analyzed when operating in the FMCW and CW Doppler modes. Finally, the conclusions are presented in Section IV.

II. DESIGN OF A HYBRID RADAR SENSOR

In [12], we proposed a hybrid radar sensor with FMCW and CW Doppler radar modes as a new monitoring method to measure the velocity of a projectile moving within the circular tube of an SRS system, as shown in Fig. 1. This was designed and developed for the soft recovery of a 155 mm test projectile launched at a supersonic speed with a 179 m compression decelerating tube. Herein, we describe its implementation and experimental verification. The design of each component is discussed in the following sections.

A. PRINCIPLE

The circular tube of the SRS shown in Fig. 1 comprises a circular metal pipe with a diameter of 155.8 mm to guide a 155 mm bullet. It is crucial to select an operating frequency that enables the radar signal to exist within the circular tube. For this purpose, a circular tube was modeled as a circular waveguide, as shown in Fig. 2, and the attenuation characteristics [16] of each mode in the circular waveguide were calculated. The lowest metallic conductivity of the circular tube of the SRS (material SNCM439, metallic conductivity (σ) = 1,818,182 [17] to 4,350,096 S/m [18]) was applied, and the attenuation characteristics for the dominant mode, TE11, and the three higher-order modes were plotted.

In Fig. 2, it is shown that the operating frequency for single-mode operation within the circular tube of the SRS should be selected between $f_{C,TE11} = 1.1334$ GHz and $f_{C,TM01} = 1.4807$ GHz. A frequency of 1.4 GHz was selected in this study.

Considering the radar sensor proposed in this study is operated within a circular waveguide, unlike radars operated in free space, the transmission velocity is not equal to the

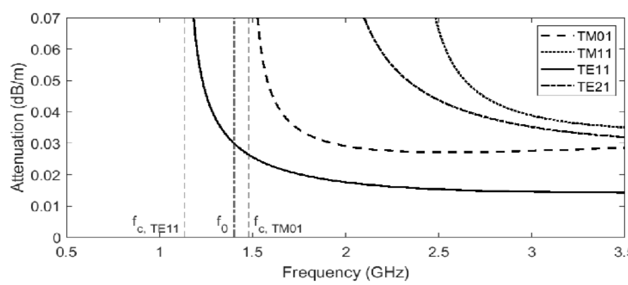

FIGURE 2. Attenuation of various modes in a tube (circular waveguide with a = 155.8 mm, conductivity of metal = 1,818,182 S/m).

speed of light but the group or phase velocity in the tube [19]; the radar equation must be modified to consider this principle. In addition, because the metal diaphragm and piston block certain sections, errors may occur in modeling a circular tube as a perfectly circular waveguide before launch and when the projectile is prior to the initial diaphragm position.

However, because the distance to the diaphragm is large compared to the diameter of the round tube, and it is open in the direction of the gun barrel, the influence of additional resonant modes is considered negligible [20].

1) FMCW RADAR MODE

In the proposed hybrid radar sensor, the FMCW radar was used to determine the position of the projectile after firing. As the CW Doppler radar cannot measure the distance if the target does not move, another sensor that can measure the distance using common hardware was designed. On the other hand, the FMCW radar can also measure the velocity, i.e., the Doppler signal; however, it has the limitation that the projectile inside the SRS has the fastest velocity at a distance of zero meters, which inevitably leads to a region with negative intermediate frequency (IF) values. This requires complex circuits and signal processing to solve the Doppler ambiguity in measuring the velocity of the initial projectile. Therefore, we attempted to implement a hybrid sensor that can operate as both radar sensors in one system, primarily because the desired goals cannot be realized by operating the FMCW radar and CW Doppler radar alone.

The distance equation for an FMCW radar with triangular wave modulation in free space is given by (1) [21].

$$D_{p0} = (c \times f_b)/(4 \times f \times f_m), \tag{1}$$

where c (m/s) is the speed of light in free space, 2.998×10^8 m/s, f_b(Hz) is the received beat frequency, f is the frequency bandwidth of the FMCW radar, and f_m(Hz) is the triangular modulation frequency.

Because the FMCW mode of the proposed monitor sensor operates within a circular waveguide, the speed of light in free space should be substituted by the speed in the tube ($\lambda_{g,TE11} \times f_0$), as shown in (2).

$$D_p = (\lambda_{g,TE11} \times f_0 \times f_b)/(4 \times f \times f_m), \tag{2}$$

where, the guide wavelength $\lambda_{g,TE11}$ in TE11 mode of the circular waveguide is given by

$$\lambda_{g,TE11} = 2\pi/\sqrt{k_0^2 - \left(p'_{TE11}/a\right)^2}, \tag{3}$$

k_0^2 is the wave number in free space, p'_{TE11} is the propagation constant of the TE11 mode in a circular waveguide, and a is the radius of the SRS tube, i.e., the radius of the circular waveguide [16], [21].

2) CW DOPPLER RADAR MODE

Another CW radar mode of the proposed hybrid radar sensor was used to measure the projectile traveling velocity. In a typical CW Doppler radar, velocity V_{p0} (m/s) of the projectile is expressed as a function of wavelength λ_0 in free space and Doppler frequency f_d (Hz), as shown in (4) [21].

$$V_{p0} = (\lambda_0 \times f_d)/2. \tag{4}$$

Because the proposed radar sensor is operated inside a circular waveguide excited in TE11 mode, the wavelength λ_0 in free space should be replaced by the guide wavelength $\lambda_{g,TE11}$ in (3) and changed as shown in (5).

$$V_p = (\lambda_{g,TE11} \times f_d)/2. \tag{5}$$

The velocity of the projectile can be calculated from the Doppler signal measured inside the circular tube using (5), from which the distance and deceleration can be calculated.

B. FEEDER

The feeder was designed to ensure that the TE11 mode was properly fed into the circular tube at the selected operating frequency, as shown in Fig. 3. A coaxial line feeder protruding from the inner side of the circular tube could not be applied to this sensor because it interfered with the movement of the projectile in the circular tube of the SRS. Additionally, a protective cover may be required to prevent the entry of gunpowder dust generated during firing.

Considering these situations, a rectangular waveguide was selected and attached to the aperture, and the coaxial line was fed into this rectangular waveguide. In detail, at the junction of the feeder and SRS tube (cross-section (a) in Fig. 3), the E-field of the TE10 mode, the main mode of the rectangular waveguide, is parallel to the y-axis, whereas inside the SRS device (cross-section (b) in Fig. 3), the E-field of the TE11 mode, the main mode of the circular waveguide, is excited parallel to the y-axis, such that radio waves can be transmitted without interfering with the projectile motion.

The detailed design parameters of the rectangular wave feeder are shown in Fig. 4, and the design values of each part

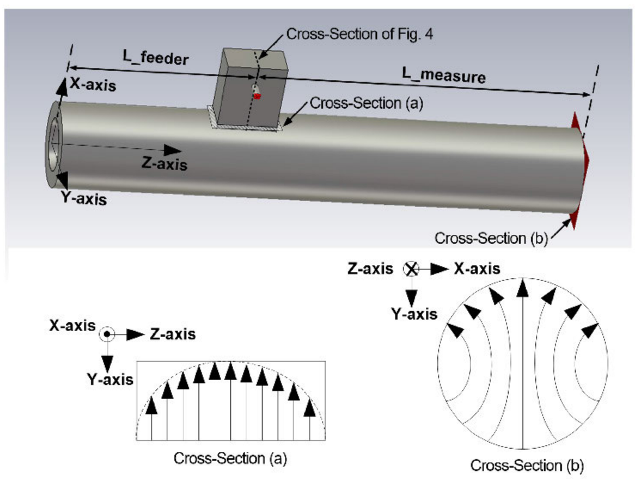

FIGURE 3. Feeder installation and the excited modes on the feeder joint and SRS tube.

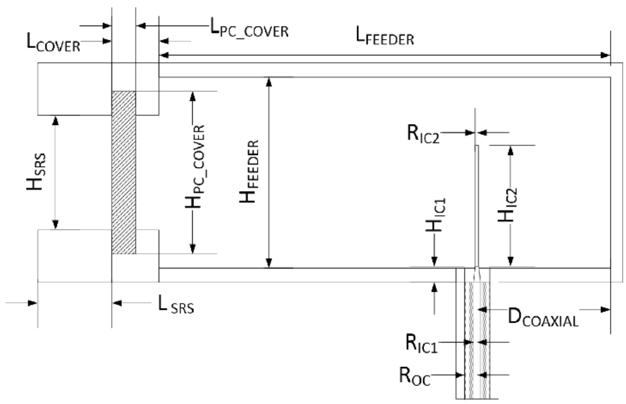

FIGURE 4. Configuration of the feeder.

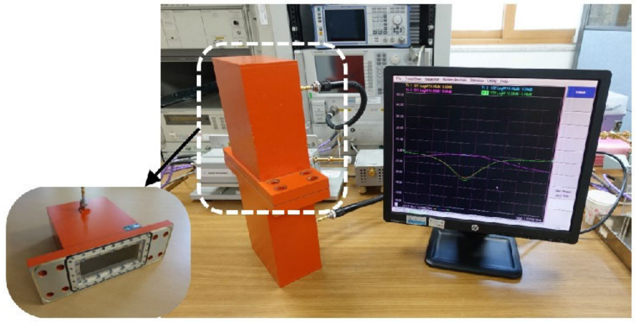

FIGURE 5. Fabricated feeder and the back-to-back experimental configuration for the S-parameter measurement.

TABLE 1. Design parameters of the feeder.

Contents	Design Values (λ0)	Contents	Design Values (λ0)
W_{SRS}	0.630	W_{FEEDER}	0.770
H_{SRS}	0.233	H_{FEEDER}	0.385
L_{SRS}	0.150	L_{FEEDER}	0.909
L_{COVER}	0.093	R_{OC}	0.024
W_{PC_COVER}	0.723	R_{IC1}	0.007
H_{PC_COVER}	0.327	H_{IC1}	0.032
L_{PC_COVER}	0.047	R_{IC2}	0.003
$D_{COAXIAL}$	0.269	H_{IC2}	0.243

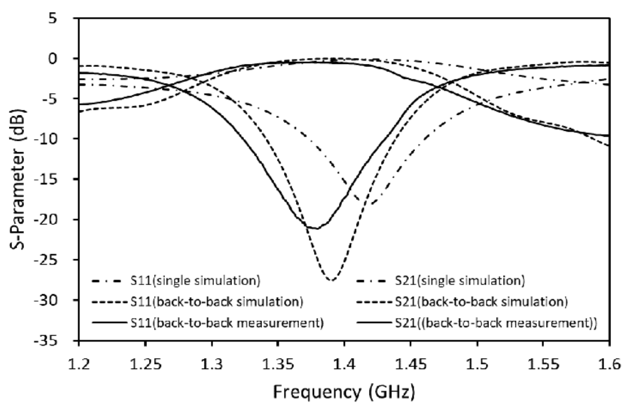

FIGURE 6. S-parameter results of the feeder.

are listed in Table 1. The fabricated feeder is shown in Fig. 5. Its reflection coefficient (S11) and insertion loss (S21) were measured via a back-to-back measurement method using a network analyzer, as shown in Fig. 5. These characteristics are similar to the analysis results obtained using the CST STUDIO SUITE™, as depicted in Fig. 6.

C. HYBRID RADAR SENSOR

The proposed hybrid radar sensor was designed, as shown in Fig. 7, based on the patent in [12]. Ref_OSC was generated by bandpass filtering the signal through a phase-locked loop (PLL). Center frequency f0 was generated using a direct digital synthesizer (DDS). Using a divider, half of the signal was sent to the amplifier, low-pass filter (LPF), combiner, and finally to the feeder. We used a combiner instead of a circulator here because the lower cost and the robustness against the shockwaves from artillery fire. At this time, through DDS control using a digital signal processor (DSP), the transmitted signal and local oscillator signal of the In-phase and quadrature (IQ) mixer were generated as an FMCW or a CW signal such that it could be independently operated in two modes. The signal transmitted from the feeder to the circular tube was reflected by the target, then it was received. The received signal was shifted by a beat frequency proportional to the projectile position (distance) in the FMCW operation mode or by a Doppler frequency generated by the projectile velocity in the CW Doppler operation mode. In the FMCW mode, a triangular modulation with f_m of 400 Hz was used, and f was set at 70 MHz.

The received signal for each mode was passed through a bandpass filter (BPF), amplified by an amplifier, separated into IF band I/Q signals in an IQ mixer, and input to the analog-to-digital converter (ADC) of a DSP.

The converted signal was delivered to the control room PC via RS422 communication such that the data could be recorded. The stored signal was post-processed to calculate the speed and position of the projectile in the tube. When a user selects the mode of the hybrid sensor in the control program of the control PC, the control PC remotely controls the DSP via RS422 communication to change the signal generated by the DDS to operate in either the FMCW mode or the CW radar mode.

Fig. 8 shows the monitor sensor fabricated based on the design shown in Fig. 7. The monitoring sensor was connected to a feeder mounted on the SRS tube using a cable via an n-type connector.

Unlike onboard measuring devices, the proposed hybrid radar sensor can be used semipermanently. The in-track velocity of the projectile could be measured at any time without having to spend a significant amount of time disassembling the device from the projectile after the test or

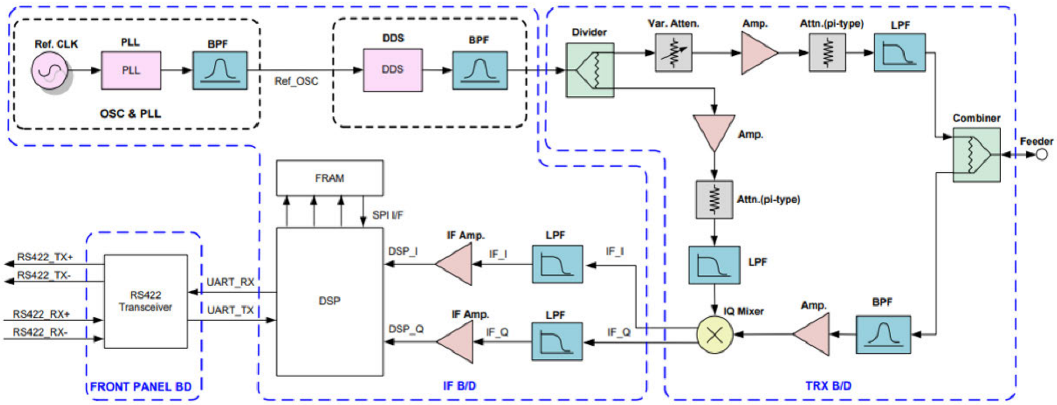

FIGURE 7. Block diagram of the monitor sensor.

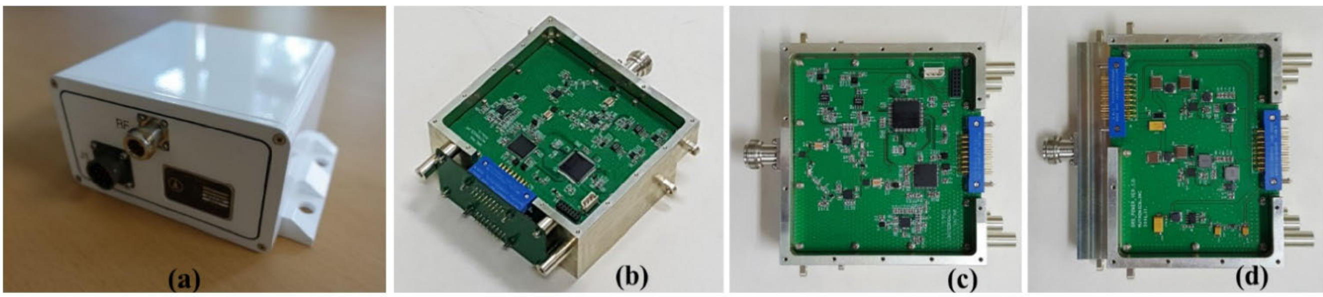

FIGURE 8. Fabricated monitor sensor: (a) Full configuration: Inside view of the monitor sensor, (b) side view, (c) top view, and (d) bottom view.

verifying the signal. Additionally, the FMCW mode was used to estimate the location of the test projectile in the SRS device without performing a manual visual check after the test. This has the advantage of significantly reducing the preparation time for the next test, even if the projectile is not retrieved normally from the SRS device during the test and is stuck in the tube.

The proposed monitoring sensor has the disadvantage of being unable to directly measure the deceleration of the test projectile as an onboard measurement. However, in the SRS test at the operational stage, instead of at the test facility installation stage, the proposed monitoring sensor is useful because only accurate velocity information is sufficient to determine whether soft recovery is performed normally.

III. RESULT

A. FEEDER TEST AFTER THE INSTALLATION ON THE SRS

The feeder was designed and fabricated, as described in the previous section. As shown in Fig. 9, the feeder was mounted in the fabricated tube before installation in the SRS testbed, and the transmission path loss characteristics were measured.

Because the physical length of the tube was too long for a two-port measurement, a one-port measurement method was used, which utilizes the characteristic that when port 2 is shorted, half of the reflection coefficient value at port 1 becomes the transmission path loss.

To verify the transmission loss with distance, a metal plate for shorting was attached to various positions inside the fabricated tube, and the magnitude of the reflected signal was measured using the time transform function of the network analyzer, as depicted in Fig. 10. Half of the first peak value was considered as transmission loss. The measurement results are presented in Fig. 11. As illustrated in Fig. 11, the measurement results show a path loss of 0.1772 dB/m, which is substantially larger than the 0.0300 dB/m calculated using the electrical conductivity of SNCM439, as shown in Fig. 2.

To analyze the reason for the large difference between the calculated and measured values, the commercial analysis tool, STUDIO SUITE™from CST, was employed to model the structure and simulate the transmission loss. When the electrical conductivity of the lossy material Steel-1008 in the internal library of the analysis software was adjusted to the electrical conductivity value (σ = 1,181,182 S/m) of SNCM439 used in Fig. 2, the simulated transmission loss was 0.04113 dB/m, which is similar to the calculated value. After adjusting the electrical conductivity to have a similar transmission loss to the measurement, σ = 74,800 S/m has the most comparable path loss to the measurement. However, the value is too low for the electrical conductivity of the metal; therefore, it is unlikely to be the cause of the difference between the calculated and measured values. By adding the smoke vent tube (SVT) structure shown in Fig. 1 to the

FIGURE 9. Feeder test.

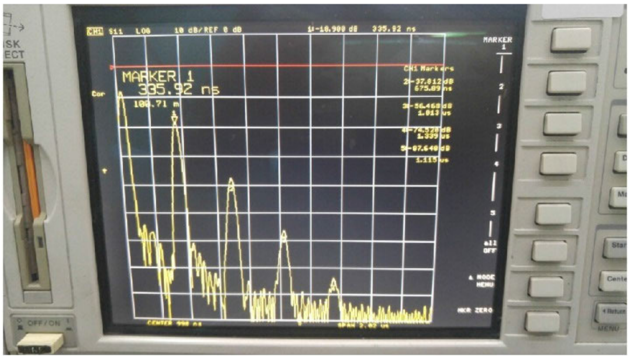

FIGURE 10. Measured result at 30 m test condition.

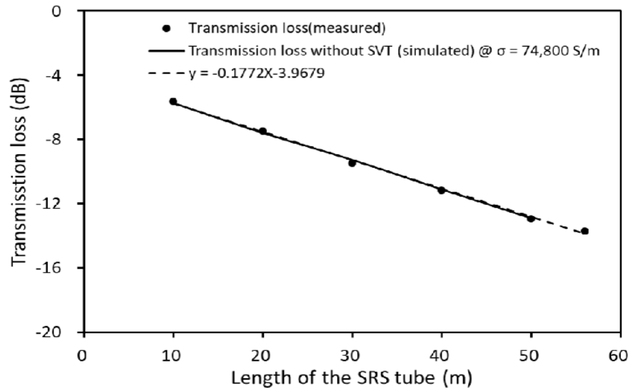

FIGURE 11. Transmission loss versus the length of the SRS tube (L_measure in Fig. 3) in the feeder tests.

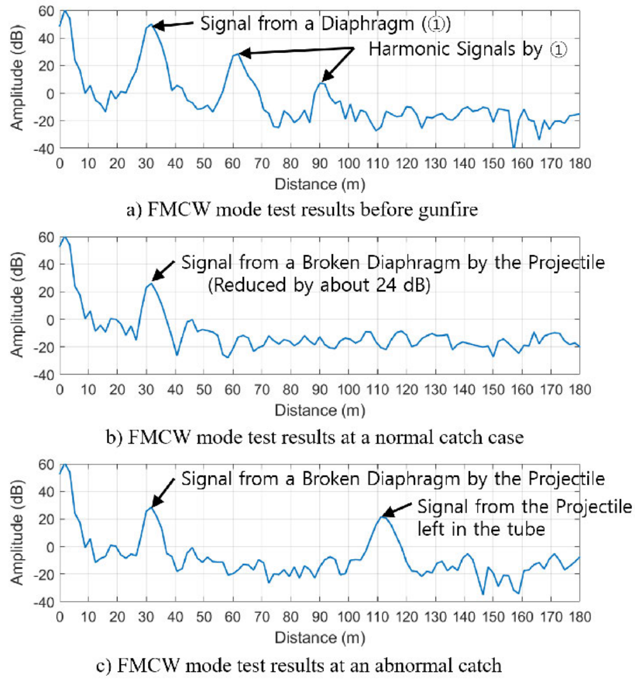

FIGURE 12. FMCW mode test results of the hybrid radar sensor.

analyzed structure shown in Fig. 2 ($\sigma = 1{,}181{,}182$ S/m), we observed that the path loss increased to 0.07029 dB/m, which is still far from the measured value.

In practical measurements, the SRS tube is not a single tube but a combination of sections of different lengths; therefore, an additional insertion loss at the intermediate joints must be considered. Moreover, the number of joints increases with the measurement distance; therefore, the insertion loss of these joints causes a difference in the path loss values between the calculation and measurement. Based on the difference between the measurement and analysis, the insertion loss of the joint was calculated to be approximately 0.64146 dB. This is a relatively large value for the junction loss, but it can be expected in a real waveguide junction.

Based on the measured path loss, the total loss of the 164 m region of the 179 m SRS device that is operated as a real waveguide is approximately 29 dB. Therefore, if the dynamic range of the monitor sensor is at least 58 dB, there should be no problem in measuring the signal at the end of the tube.

B. FIRE TEST AFTER THE INSTALLATION ON THE SRS

The data measured from the SRS device operation using the designed monitoring sensor are shown in Fig. 12.

In the FMCW operation mode, the measured signal immediately before the gunfire is shown in Fig. 12(a). A peak signal is visible owing to the reflection from the diaphragms, which are approximately 30 m apart. When the gun is fired and the projectile is normally softly recovered by the SRS device or rests on the recovery wall, a signal, as shown in Fig. 13(b), is measured. Therefore, the FMCW mode waveform after the test can indicate that the test projectile was in a soft recovery position or on the recovery wall. When the test projectile was not in the soft recovery position and was stuck in the middle of the tube, the signal was visible at a specific location, as shown in Fig. 12(c). Fig. 12(c) shows an example of the signal measured when the test shell was retrieved from a high-pressure tube (HPT) at 111 m. This phenomenon occurs when the pressure and fill conditions of the SRS test apparatus are incorrect. Therefore, the result can be used to adjust the conditions for the next test. Additionally, the precise position of the projectile can be determined, which has the advantage that the test projectile can be removed from

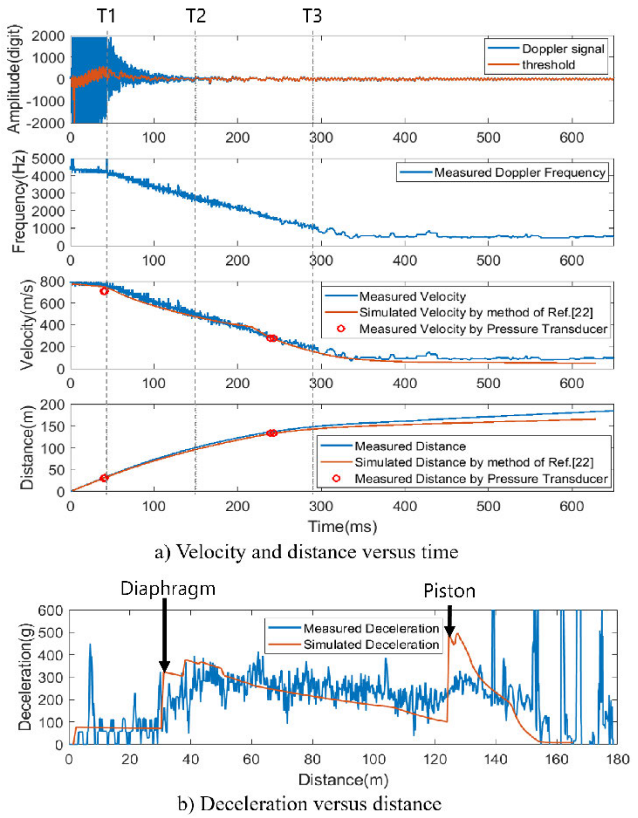

FIGURE 13. CW mode test results of the hybrid radar sensor.

a single-tube disassembly, minimizing the time between tests. Therefore, the FMCW mode can be used to verify the proper installation of the diaphragm before the test and determine the position of the projectile after the test.

The continuous wave (CW) Doppler radar mode was used to determine the velocity and deceleration of the projectile traveling through the SRS tube, as shown in Fig. 13.

First, the Doppler signal was acquired in real time, as displayed in the top plot of Fig. 13(a), and then it was postprocessed to calculate the Doppler frequency, as depicted in the second plot of Fig. 13(a), from which the projectile velocity was calculated, as illustrated in the third plot of Fig. 13(a), using (4). Furthermore, integrating the calculated projectile velocity yielded the distance traveled, as shown in the bottom plot in Fig. 13(a). The deceleration characteristics obtained by differentiating the projectile velocities are presented in Fig. 13(b).

The calculated projectile velocity and distance were almost the same as the results of the analysis method in [22] using data from the pressure sensor mounted on the SRS. The deceleration results are also similar to those obtained using the analysis method in [22], confirming that the proposed hybrid radar sensor can effectively calculate the projectile velocity, distance, and deceleration values.

Various methods exist for calculating the frequency by post-processing the Doppler signal in the CW Doppler radar mode: moving Fast Fourier transform (FFT), Kalman filter, etc. In this study, we choose the threshold-crossing method, which enables fast calculations. When the threshold is set as the result of a fixed moving average window function, the Doppler frequency calculation becomes inaccurate in the region of 300 ms or more, as shown in Fig. 14.

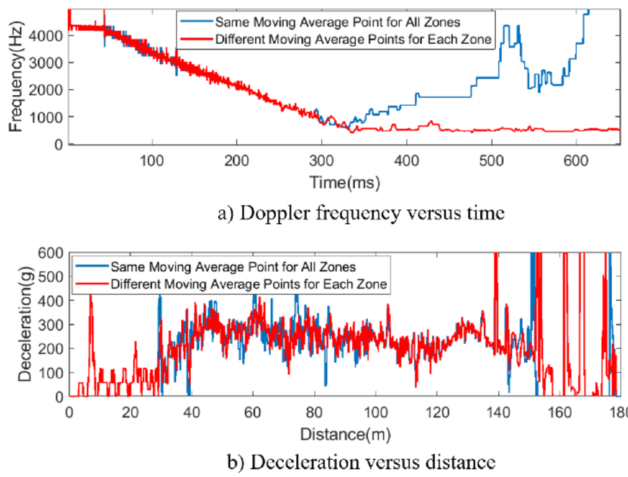

FIGURE 14. CW mode test results of the hybrid radar sensor.

To solve this problem, the most accurate frequency can be calculated by selecting sections and performing a moving average with different points in each section. In this study, the frequency was calculated using the zero-crossing method with divided zones [T1, T2, T3] = [32.71 ms, 96.14 ms, 142.5 ms] and the thresholds based on the moving average value of 80 points for 0 ∼ T1, 150 points for T1 ∼ T2, 80 points for T2 ∼ T3, and 120 points for T3 and above, respectively. If the calculated Doppler frequency changed rapidly by more than 30% of the previous value, it was treated as an abnormal value and set to the previous result.

C. DISCUSSION

The results of an artillery firing test conducted on an SRS equipped with the proposed hybrid sensor confirmed the feasibility of the proposed monitoring sensor.

The FMCW mode was used immediately after the test to confirm whether the projectile recovered normally (Fig. 12(b)) or abnormally (Fig. 12(c)). This result enabled us to immediately determine whether to retrieve the projectile from the water spout tube or wedge breaker, prepare for the next test, dismantle the tube at the identified anomalous retrieval location, and adjust the pressure conditions in the HPT and amount of water in the water-filled tube (WFT) to perform the subsequent test. This demonstrates that the proposed sensor can reduce the time between tests.

The Doppler signal was normally measured for a projectile moving in a tube, and the projectile speed, distance traveled, and deceleration were accurately calculated from the measured Doppler signal. It requires a considerably shorter time than that required to disassemble the projectile to check the recorder results after the test when using a conventional onboard recorder. Furthermore, unlike systems that use separate receivers or reflectors for measurements, which can be damaged in front of the muzzle, the SRS system is semipermanent and easy to use because it can be operated by attaching only a feeder to the side of the SRS tube.

These test results show that the calibration of (2) and (4) to the operating conditions in the circular waveguide was achieved, and the proposed hybrid sensor with FMCW and CW Doppler radar modes operated well in the circular tube, as intended.

In the CW Doppler radar, it is necessary to adjust the spacing and moving average windows for firing conditions, such as muzzle velocity change. We are yet to implement a single automatic processing algorithm that adapts to firing conditions.

The proposed monitoring sensor has a limitation in that the accuracy of the test projectile deceleration is significantly lower than that of the existing system because it is indirectly calculated from the measured Doppler frequency, unlike the conventional onboard measurement system, which directly measures the acceleration sensor.

IV. CONCLUSION

In this study, we proposed a hybrid radar sensor capable of semipermanent, near-real-time monitoring of the behavior of a projectile moving in a circular SRS tube. As the proposed sensor measures in a circular tube with a diameter of 155.8 mm, 1.4 GHz was chosen as the operating frequency, at which only the dominant mode can exist in the tube. A suitable feeder was designed to excite the dominant mode in the tube without interfering with the launched projectile. The feeder test performed after installation on the SRS showed good propagation.

The proposed hybrid radar sensor contains FMCW and CW Doppler radar modes. To accurately predict the parameters in each mode, the radar equations in free space were calibrated to the operating conditions of the circular tube.

In the FMCW radar mode, the position of the diaphragm before the firing test and the position of the projectile after the test could be accurately located, which effectively reduced the time between tests. In the CW Doppler radar mode, the projectile velocity, distance traveled, and deceleration were accurately estimated compared to previous analysis results. Additionally, compared to the conventional onboard recorder, the proposed method is faster and simpler.

The method proposed in this paper can be tested without any modification of the test projectile and has the advantage that it can be applied not only to the impact resistance test of several components mounted inside the test projectile but also to the test of actual smart ammunition.

In the future, we plan to establish an optimal signal-processing technique through further analyses of various test data, such that the system can adapt to various firing conditions.

ACKNOWLEDGMENT

The authors would like to thank Editage (www.editage.co.kr) for English language editing.

REFERENCES

[1] D. S. Somasundaram, M. B. Trabia, B. O'Toole, and Q. Liu, "Shock mitigation for electronic boards within a projectile," *Int. J. Comput. Methods Experim. Meas.*, vol. 1, no. 4, pp. 416–439, 2013.

[2] V. Chakka, M. B. Trabia, B. O'Toole, S. Sridharala, S. Ladkany, and M. Chowdhury, "Modeling and reduction of shocks on electronic components within a projectile," *Int. J. Impact Eng.*, vol. 35, no. 11, pp. 1326–1338, Nov. 2008.

[3] T. Myers, D. Geissler, B. Ellis, J. A. Cordes, and J. Vega, "Statistical comparison between component level and system level testing for the Excalibure projectile," in *Proc. 23rd Int. Symp. Ballistics*, Tarragona, Spain, 2007, pp. 605–612.

[4] J. A. Cordes, J. Lee, T. L. Myers, G. Hader, L. Reinhardt, C. Kessler, N. Gray, and M. A. Guevara, "Statistical comparisons between qualification tests for gun-fired projectiles," *J. Appl. Mech.*, vol. 77, no. 5, pp. 1–6, Sep. 2010.

[5] D. T. Chung, I. S. Rhee, B. J. Joo, D. H. Jin, O. K. Rim, and K. J. Park, "Development of a soft recovery system of supersonic projectiles," *Eng. Trans.*, vol. 60, no. 1, pp. 3–14, Sep. 2012.

[6] R. N. Teng, "Ballistic compression decelerator," U.S Patent 3 678 745, Jul. 25, 1972.

[7] A. Birk, D. Carlucci, C. McClain, and N. Gray, "Soft recovery system for 155 mm projectiles," in *Proc. 23rd Int. Symp. Ballistics, Launch Dyn.*, Tarragona, Spain, 2007, pp. 591–596.

[8] W. Zhang, L. Chen, J. Xiong, and Y. Ma, "Ultra-high G deceleration-time measurement for the penetration into steel target," *Int. J. Impact Eng.*, vol. 34, no. 3, pp. 436–447, Mar. 2007.

[9] D. J. Frew, M. J. Forrestal, and J. D. Cargile, "The effect of concrete target diameter on projectile deceleration and penetration depth," *Int. J. Impact Eng.*, vol. 32, no. 10, pp. 1584–1594, Oct. 2006.

[10] Y. Peng, H. Wu, Q. Fang, and Z. Gong, "Deceleration time of projectile penetration/perforation into a concrete target: Experiment and discussions," *Adv. Structural Eng.*, vol. 22, no. 1, pp. 112–125, Jan. 2019.

[11] M. Liennard, O. Chevalier, A. Langlet, Y. Guilmard, and M. Mansion, "An analysis of the accelerations of a projectile in a gun tube by direct measurements and telemetry of the data," *Mech. Ind.*, vol. 19, no. 4, p. 406, 2018.

[12] J. H. Choi, M. S. Song, and J. E. Roh, "Deceleration hysteresis measuring apparatus for soft recovery system," U.S Patent 9 875 633 B1, Jan. 23, 2018.

[13] H. Boeglen, L. Barbero, A. Traore, D. Schmoltzi, and R. Vauzelle, "Analysis of the Doppler behavior on a supersonic speed ground-projectile channel," in *Proc. 10th Eur. Conf. Antennas Propag. (EuCAP)*, Apr. 2016, pp. 1–5, doi: 10.1109/EuCAP.2016.7481252.

[14] M. Schneider, D. Eckenfels, and S. Nezirevic, "Doppler-radar: A possibility to monitor projectile dynamics in railguns," *IEEE Trans. Magn.*, vol. 39, no. 1, pp. 183–187, Jan. 2003, doi: 10.1109/TMAG.2002.805956.

[15] S. Myers and R. Zapata-Ramos, "Application of W-band, Doppler radar to railgun velocity measurements," *Proc. Eng.*, vol. 58, pp. 369–376, Jan. 2013.

[16] D. M. Pozar, *Microwave Engineering*, 2nd ed. Hoboken, NJ, USA: Wiley, 1981, pp. 132–141.

[17] *SNCM439 Data*. Accessed: Nov. 3, 2023. [Online]. Available: https://www.steelgr.com/Steel-Grades/Carbon-Steel/sncm439.html

[18] *SNCM439(AISI 4340) Data*. Accessed: Nov. 3, 2023. [Online]. Available: https://www.makeitfrom.com/material-properties/Annealed-4340-Ni-Cr-Mo-Steel

[19] S. Ramo, J. R. Whinnery, and T. V. Duzer, *Fields and Waves in Communication Electronics*, 3rd ed. Hoboken, NJ, USA: Wiley, 1993, pp. 262–263.

[20] M. I. Skolnik, *Introduction to Radar Systems*, 2nd ed. New York, NY, USA: McGraw-Hill, 1981.

[21] Class Handout. *Resonant Cavities and Waveguides*. Accessed: Nov. 3, 2023. [Online]. Available: https://web.mit.edu/22.09/ClassHandouts/CHAP12.PDF

[22] M. Song and J. Kim, "Numerical studies on the deceleration characteristics of supersonic projectile according to the test condition parameters in a soft recovery system," *J. Korea Inst. Mil. Sci. Technol.*, vol. 23, no. 5, pp. 485–493, Oct. 2020.

MYUNG-SUK JUNG received the B.S. degree in electronics and electrical engineering from Kyungpook National University, Daegu, South Korea, in 1999, and the M.S. degree in electronics and electrical engineering from the Pohang University of Science and Technology (POSTECH), Pohang, South Korea, in 2001, where she is currently pursuing the Ph.D. degree.

She has been a Principal Researcher with the Agency for Defense Development, Daejeon, South Korea, since 2001. Her current research interest includes development of the microwave and millimeter-wave sensors.

JAE-HYUN CHOI received the B.S. and M.S. degrees in electronics and the Ph.D. degree in radio engineering from Chungnam National University, Daejeon, South Korea, in 1995, 1997, and 2014, respectively.

Since 1998, he has been a Principal Researcher with the Agency for Defense Development (ADD), Daejeon. His research interests include miniaturized transceivers for small radars at close range and millimeter-wave (MMW) radar/radiometer for various fuzing systems.

MIN-SUP SONG received the B.S. degree in mechanical engineering from Chungnam National University, Daejeon, South Korea, in 2003, and the M.S. degree in mechanical engineering from the Korea Advanced Institute of Science and Technology (KAIST), Daejeon, in 2005, where he is currently pursuing the Ph.D. degree in mechanical engineering. He has been a Senior Researcher with the Agency for Defense Development, Daejeon, since 2012. His current research interest includes structural design development.

JIN-EEP ROH received the B.S. degree in electronics and electrical engineering from the University of Ulsan, Ulsan, South Korea, in 1984, and the M.S. degree in electronics engineering and the Ph.D. degree in information and communication engineering from Chungnam National University, Daejeon, South Korea, in 1993 and 2007, respectively.

Since 1984, he has been a Principal Researcher with the Agency for Defense Development, Daejeon, where he has also been responsible for the design and development of the transceiver for proximity-fuze sensors. His current research interest includes miniaturized transceivers for small radars at close range for various fuzing systems.

KYUNG-TAE KIM (Member, IEEE) received the B.S., M.S., and Ph.D. degrees in electrical engineering from the Pohang University of Science and Technology (POSTECH), Pohang, South Korea, in 1994, 1996, and 1999, respectively.

From 2002 to 2010, he was a Faculty Member with the Department of Electronic Engineering, Yeungnam University. Since 2011, he has been with the Department of Electrical Engineering, POSTECH. From 2012 to 2017, he was the Director of the Sensor Target Recognition Laboratory, sponsored by the Defense Acquisition Program Administration and the Agency for Defense Development. He is currently a Professor. He is also the Director of the Unmanned Surveillance and Reconnaissance Technology (USRT) Research Center and the Next Generation Imaging Radar System Research Center, POSTECH. He is the Director of the Next Generation Defense Multidisciplinary Technology Research Center and the Graduate School of Defense Science and Technology Program, POSTECH. He is the author of more than 350 articles in journals and conference proceedings. He is carrying out several research projects funded by the Korean Government and several industries. His research interests include radar imaging (SAR/ISAR), machine learning of radar signatures, detection/estimation/tracking, the direction of arrival, micro-Doppler analysis, digital beamforming, electronic warfare, electromagnetic scattering, the indoor monitoring of individuals, and sensor fusion. He is a member of KIEES. He was a recipient of several outstanding research awards and best paper awards from the Korea Institute of Electromagnetic Engineering and Science and international conferences.